DOI: 10.1021/ma101418e

Macromolecules
ARTICLE

Nanostructure Evolution during Photopolymerization in Lyotropic Liquid Crystal Templates

Bradley S. Forney and C. Allan Guymon*

Department of Chemical and Biochemical Engineering, the University of Iowa Iowa City, Iowa 52242

Received June 25, 2010; Revised Manuscript Received August 23, 2010

ABSTRACT: The ability to direct polymer structure on the nanometer scale has provided access to enhanced material properties that may be tailored to accommodate a growing number of advanced biological and industrial applications. A promising method of generating nanostructure in organic polymers uses self-assembling lyotropic liquid crystalline (LLC) mesophases as templates for polymerization. Unfortunately, thermodynamically driven phase separation often prevents polymer morphology from being precisely controlled. As the demand for polymers with accurately engineered properties increases, a detailed understanding of the phase separation process is needed to control the nanostructure and properties of LLC templated polymers. In this study, photopolymerization kinetics are utilized to identify phase separation events occurring during the photopolymerization of poly(ethylene glycol) diacrylate and hexanediol diacrylate monomers templated in the normal hexagonal or lamellar LLC mesophases. Discontinuities are found in the polymerization rate of anisotropic polymers at several double bond conversions that are not present in the rate profiles of isotropic controls. The polymer morphology was subsequently characterized at particular conversions using small angle X-ray scattering. Changes in polymer nanostructure occur at double bond conversions that coincide with the observed rate discontinuities. These results demonstrate that photopolymerization kinetics can be used as a probe to monitor the evolution of polymer nanostructure during polymerization and optimize the conditions governing the control of polymer morphology to enhance properties dependent on nanostructure.

Introduction

Polymers with nanometer size morphologies are generating significant research interest due to their potential application in areas including tissue engineering, controlled release, and size-selective separation media.[1−3] Of particular importance is the potential to improve and tune physical properties by controlling polymer nanostructure as properties ranging from mechanical strength to permeability are highly dependent on local order and size of morphological features.[4] For example, polymers with submicrometer morphologies have exhibited greater compressive moduli, swelling, permeability, and biological interaction than their isotropic counterparts.[5−8] Furthermore, these properties have been tuned by modifying polymer morphology while maintaining the original polymer chemistry. These characteristics could be used to engineer biomedical devices such as tissue scaffolds and hydrogels with the proper mechanical, degradative, and swelling properties needed for successful performance using well-characterized biopolymers.[9]

Methods of directing polymer morphology may use templates to segregate monomers into the desired geometry followed by polymerization to transfer the template structure to the polymer.[10−12] One promising method of generating nanostructure in organic polymers uses self-assembling lyotropic liquid crystals (LLCs) as templates for polymerization.[13] LLCs are typically low molecular weight surfactants that can self-assemble into a variety of nanometer size mesophases in the presence of a solvent such as water. The highly ordered LLC mesophases are used to segregate monomers into a variety of different geometries by utilizing the inherent water- and oil-soluble domains. In fact, the polar and nonpolar domains of LLC templates have been used to compatibilize otherwise immiscible hydrophobic and hydrophilic monomers, allowing properties intermediate of each polymer to be incorporated into the final polymer network.[14] LLC mesophases are particularly well-suited for templating applications because their morphology and characteristic length depend primarily on the concentration, polarity, and size of surfactant molecules, thus providing a facile method of altering polymer nanostructure.[15]

The synthesis of LLC templated polymers is relatively simple and their large-scale production is expected to be more feasible than other templating methods.[16] Ideally, the template can be used to precisely control polymer morphology on the desired size scale during polymerization.[17] In practice, however, it is often difficult to control polymer structure throughout the polymerization reaction. Thermodynamically driven phase separation often occurs as monomer is converted to polymer and frequently yields polymers with poorly defined nanostructures.[18] Phase separation prevents polymer morphology from being precisely controlled and changes properties dependent on nanostructure. A detailed understanding and investigation of the evolution of polymer nanostructure during polymerization is required to determine the kinetic and thermodynamic conditions needed to precisely direct polymer nanostructure and optimize polymer properties.[19,20]

Polymer−template phase separation is a significant problem in many polymer templating strategies and often prevents the control of polymer nanostructure and properties.[18,21] The polymerization strategy and initiation method used to generate the templated polymer will often dictate the extent to which template structure is transferred to the polymer and overall success of the templating process. Factors including polymerization rate,

*Corresponding author: Telephone: +1 319 335 5015. Fax: +1 319 335 1415. E-mail: allan-guymon@uiowa.edu.

 Published on Web 09/23/2010

propagation mechanism, and local environment in which polymerization occurs must be considered when selecting a polymerization strategy.[19] Rapid initiation rates have been proposed as a method of preserving the original LLC template order by forcing the polymer to attain sufficient conversion before phase separation can occur.[22,23] Photopolymerization is a particularly attractive polymerization strategy for templated systems because the initiation rate is inherently fast, independent of temperature, and readily controlled through light intensity and photoinitiator concentration.[24−26] The temperature independent initiation rates of photopolymerization allow polymerization to be performed at the temperature at which the template is most stable and could promote the successful transfer of template structure to the polymer.[27] In addition to the advantages photopolymerization offers in generating LLC templated polymers, it is also used as a tool to probe the kinetic and structural behavior during polymerization.[28,29] Because light is used to generate the reactive center, the initiation step can be controlled temporally by regulating irradiation time, which provides a robust method of quenching the polymerization to study the relationship between conversion and polymer structure. Furthermore, the initiation rate can be easily adjusted and the impact of polymerization kinetics on polymer structure may be studied more feasibly.

Photopolymerization kinetics provide a considerable amount of information regarding the structure of LLC templated polymers during polymerization. The order imposed on monomers by the parent template significantly affects the local concentration, segregation, and diffusional behavior of reactive species.[19,23,30−35] Likewise, changes in the LLC mesophase resulting from phase separation events will alter the local concentration, segregation, and diffusional behavior of reactive species and directly impact the polymerization kinetics. Thus, polymerization kinetics are directly related to local order and may be used to elucidate changes in polymer nanostructure occurring during polymerization. Numerous studies have utilized photopolymerization kinetics to identify changes in polymer morphology by comparing the polymerization rate and kinetic constants of templated systems to those of an appropriate isotropic control.[23,30,31,34−36] When abrupt changes in kinetic constants or discontinuities in the polymerization rate are observed in the templated system and not in the isotropic control, these kinetic differences are usually attributed to alterations in the segregation and diffusional behavior of reactive species resulting from changes in polymer structure. Despite this kinetic evidence of structural changes, polymer morphology has been exclusively characterized before and after polymerization, providing limited insight into the evolution of polymer structure during polymerization.

In this study, the nanostructure of LLC templated polymers is characterized at specific conversions to better understand and direct the evolution of polymer structure. The polymerization rate of LLC-monomer systems that self-assemble into highly ordered mesophases before polymerization and phase separate during polymerization were investigated for discontinuities relative to isotropic controls. Utilizing the temporal control of photopolymerization, the polymer structure was characterized directly using X-ray scattering at conversions coinciding with irregular rate behavior. These investigations not only begin to reveal how polymer morphology evolves during polymerization but also provide methods that may be used to systematically establish how polymerization kinetics and LLC self-assembly can be optimized to control polymer structure. It is hypothesized that characterizing polymer nanostructure during polymerization will provide valuable kinetic and thermodynamic information describing the phase separation process. Such knowledge may be used to direct polymer structure and thus tailor polymer properties to accommodate a number of diverse and advanced applications.

Experimental Section

Materials. The monomers used in this study were poly(ethylene glycol) diacrylate (PEGDA, $M_n \sim 258$ Aldrich) and 1,6-hexanediol diacrylate (HDDA, Sartomer). The lyotropic liquid crystal was polyoxyethylene(10) cetyl ether (Brij 56, Aldrich). 2,2-Dimethoxy-1,2-diphenylethan-1-one (Irgacure 651, Ciba Specialty Chemicals) was used as the photoinitiator. Ethylene glycol diacetate (EGDAc, Aldrich) was also used as a solvent in this study. All chemicals were used as received.

Sample Preparation. Samples containing lyotropic liquid crystals were prepared by mixing specific concentrations of monomer, surfactant, deionized water, and photoinitiator. Isotropic samples were prepared by mixing the respective monomer with ethylene glycol diacetate and photoinitiator. All samples contained 20 wt % monomer and 0.5 wt % photoinitiator with respect to monomer mass. Sample homogeneity was achieved using centrifugation, heat sonication, and vortex mixing.

Kinetics. Photopolymerization kinetics were studied using a Perkin-Elmer differential scanning calorimeter (photo-DSC) equipped with a medium-pressure UV arc lamp (Ace Glass) to initiate polymerization. The emission spectrum was controlled using a 365 nm band-pass filter, and light intensity was adjusted with neutral density filters and by varying the distance of the sample from the lamp. Approximately 4 mg of sample was placed into crimped aluminum pans and covered with a thin transparent fluorinated ethylene propylene copolymer (Teflon FEP, DuPont) film to minimize heat loss resulting from water evaporation. Samples were heated above their clearing temperature to promote uniform thickness and thermal contact. Oxygen inhibition was suppressed by purging samples with nitrogen for 8 min prior to polymerization. Heat flow, Q, was monitored in real-time, t, by maintaining a constant sample temperature of 30 °C and used to calculate the normalized polymerization rate, R_p, using eq 1

$$R_p = \frac{\bar{R}_p}{[M]} = \frac{Q(t)\cdot MW}{n\cdot \Delta H_p \cdot m} \quad (1)$$

where $\bar{R}_p$ is the extensive polymerization rate, [M] is the monomer concentration, MW is the monomer molecular weight, n is the monomer functionality, ΔH_p is the enthalpy of polymerization, and m is the monomer mass.[37] Double bond conversion, p, was calculated by integrating the normalized polymerization rate with respect to time.

Characterization

The optical anisotropy of LLC samples was characterized before and after polymerization using a polarized light microscope (PLM, Nikon, Eclipse E600W Pol) equipped with a hot stage (Instec, Boulder, CO). PLM images were obtained by placing samples sandwiched between a glass microscope slide and coverslip on the microscope stage, heating above their clearing point, and allowing them to cool slowly at room temperature. Samples were photopolymerized with the UV light source described above. Optical textures were examined for birefringent patterns characteristic of the ordered phases formed in the LLC samples. PLM images obtained before and after photopolymerization were compared to determine the extent of phase disruption that occurred as monomers polymerized into a cross-linked network.

Polymer nanostructure was characterized with a Nonius FR590 small angle X-ray scattering (SAXS) apparatus using a standard copper target Röntgen tube with a Ni-filtered Cu Kα line of 1.54 Å as the radiation source, a collimation system of the Kratky type, and a PSD 50 M position sensitive linear detector (Hecus M. Braun, Graz). Phases were indexed by calculating the d-spacing ratios of scattering peaks. The scattering vector, q, was calculated from the angle of the scattered radiation and the X-ray wavelength. SAXS profiles were desmeared to correct for beam-height effects

using a direct transform method described elsewhere.[38] Desmeared profiles were background corrected and normalized to the invariant, J, calculated using eq 2

$$J = \int_0^\infty I(q)q^2 \, dq \tag{2}$$

where $I(q)$ is the desmeared intensity.[39] The invariant represents the scattering power of the sample, is independent of sample morphology, and is used to correct for differences in scattering volume, electron densities, and fluctuations in beam intensity.[40] In other words, normalizing the scattering profiles to the invariant allows polymer structure to be compared without having to measure absolute intensities. Additionally, the Lorentz correction was applied to correct for the differences in time that individual reciprocal lattice points spend in a diffracting position.[41]

Results and Discussion

An encouraging method of generating nanostructure in polymers uses LLC mesophases as templates for polymerization. However, thermodynamically driven phase separation typically prevents polymer nanostructure from being precisely controlled. A detailed description regarding the evolution of polymer morphology during polymerization is needed to optimize the thermodynamic and kinetic conditions necessary to accurately direct polymer nanostructure. Numerous studies have utilized photopolymerization kinetics to study polymer morphology during polymerization.[19,27,30,32,33,36] Discontinuities in polymerization rate and kinetic constants are often observed during the polymerization of LLC templated monomers and have been suggested to result from changes in local order. However, because the structure of LLC templated systems is usually characterized before and after the polymerization reaction, there is little direct evidence supporting that such kinetic behavior is due to changes in polymer structure. Herein, photopolymerization kinetics are utilized to identify changes in polymer structure occurring during polymerization to understand and control polymer−template phase separation. A complete description of the kinetic and thermodynamic factors governing the structure of LLC templated polymers could lead to the synthesis of polymers with precisely engineered physical properties.

To illustrate the effect of local order on photopolymerization kinetics, the polymerization rate of LLC-monomer samples containing 20 wt % poly(ethylene glycol) diacrylate (PEGDA) or 20 wt % 1,6-hexanediol diacrylate (HDDA) and varying concentrations of the surfactant Brij 56 in water were investigated. The impact of liquid crystalline order on polymerization kinetics is evident from the rate profiles for PEGDA polymerized in the isotropic, normal hexagonal, and lamellar mesophases (Figure 1a). The polymerization of PEGDA is fastest in the normal hexagonal mesophase formed at 40 wt % surfactant with the maximum rate being approximately a factor of 3 greater than that observed for the isotropic polymerization of PEGDA in EGDAc. As the concentration of surfactant increases to 50 wt %, the maximum polymerization rate of PEGDA is less than half of that observed at 40 wt % surfactant even though both samples have a normal hexagonal morphology before polymerization. Also, the maximum polymerization rate for PEGDA templated in the lamellar LLC mesophases formed at 60 and 70 wt % surfactant is greater than the maximum polymerization rate of PEGDA in solvent. Similar trends are observed in the rate profiles of HDDA polymerized in the isotropic, normal hexagonal, and lamellar phases (Figure 1b). The polymerization rate of HDDA is greatest in the normal hexagonal phase formed at 30 wt % surfactant and decreases with increasing surfactant concentration. For both

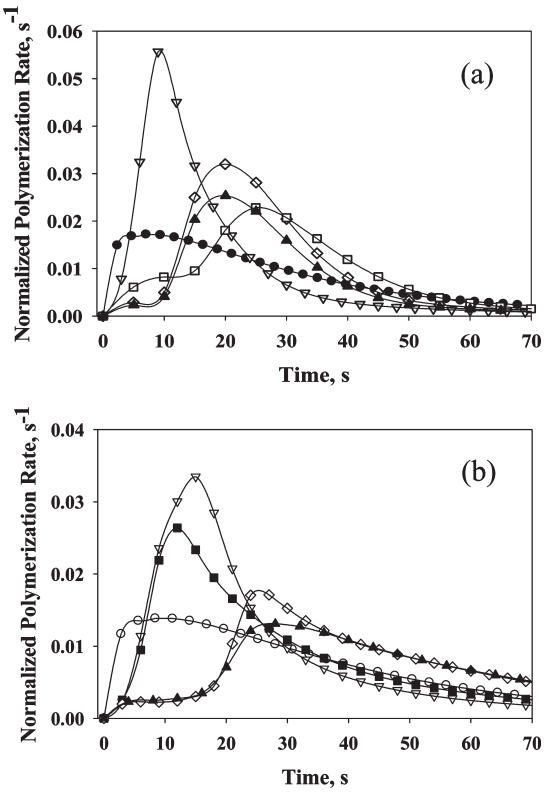

Figure 1. (a) Polymerization rate as a function of time for 20 wt % PEGDA in EGDAc (isotropic, ●), and with 40 wt % (normal hexagonal , ▽), 50 wt % (normal hexagonal, □), 60 wt % (lamellar, ◇), and 70 wt % (lamellar, ▲) Brij 56 in water. (b) Polymerization rate as a function of time for 20 wt % HDDA in EGDAc (isotropic, ○), and with 30 wt % (normal hexagonal, ▽), 40 wt % (normal hexagonal, ■), 50 wt % (lamellar, ◇), and 60 wt % (lamellar, ▲) Brij 56 in water. Polymerization was initiated with 0.5 wt % Irgacure 651 at a light intensity of 3.27 mW/cm^2.

PEGDA and HDDA monomers, the polymerization rate is faster at lower surfactant concentration within a given LLC mesophase. This behavior is likely due to a decrease in local monomer concentration at higher surfactant concentrations. This kinetic behavior has been reported for similar LLC-monomer systems and is discussed in greater detail elsewhere.[23,32,33]

It is clear from the rate profiles in Figure 1 that LLC order has a significant impact on polymerization kinetics. Interestingly, rate profiles of anisotropic samples show kinetic behavior that is much different from their isotropic counterparts. For example, a deceleration in polymerization rate is observed at low double bond conversion for both PEGDA and HDDA samples templated with 50 wt % surfactant. This behavior differs from traditional isotropic photopolymerization kinetics of diacrylate monomers in which the polymerization rate is relatively continuous.[42] These differences in polymerization rate appear to be due to the segregation of acrylate functional groups as directed by the LLC template. It has often been suggested that rate discontinuities in LLC systems result from phase separation events that alter the local concentration, segregation, and diffusional behavior of monomers. However, because polymer structure is typically characterized before and after polymerization, little structural data are available to support this hypothesis. The morphology of each system in Figure 1 was characterized before and after polymerization using PLM and SAXS to determine if a significant change in polymer structure is occurring during polymerization. With phase separation occurring during polymerization, the conversion at which polymer nanostructure changes may be identified by studying the systems photopolymerization kinetics,

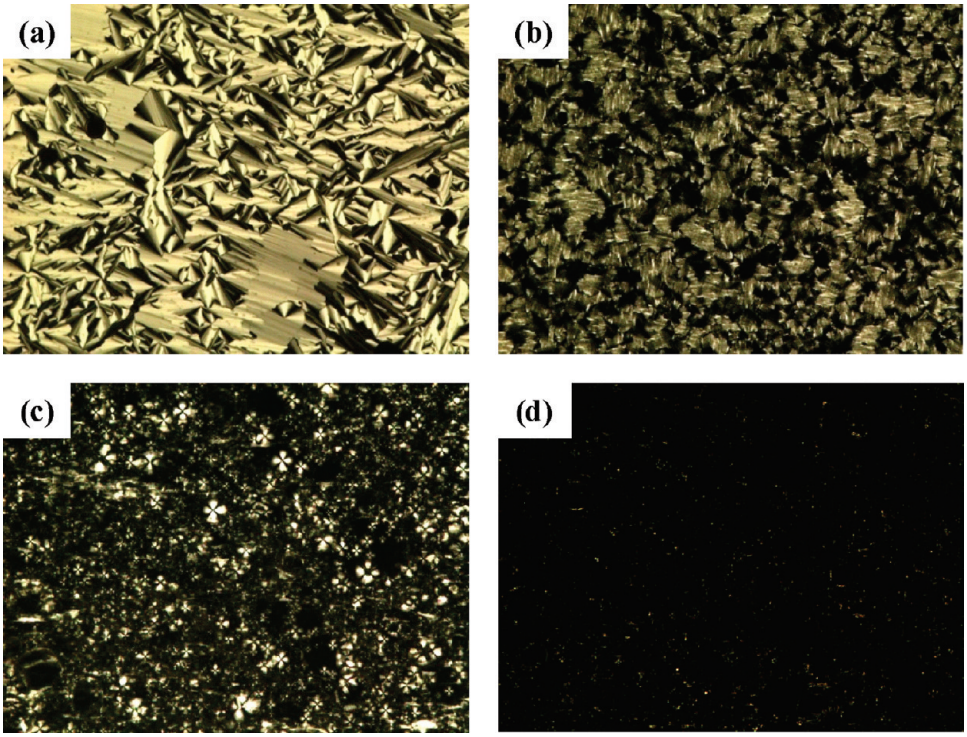

Figure 2. Polarized light micrographs of LLC templated samples before and after photopolymerization at 10× magnification. Shown are samples of 20 wt % PEGDA with 50 wt % Brij 56 in water (a) before and (b) after polymerization and a sample of 20 wt % HDDA with 50 wt % Brij 56 in water (c) before and (d) after polymerization. Polymerization was initiated with 0.5 wt % Irgacure 651 at a light intensity of 0.5 mW/cm^2.

thus providing insight into the evolution of polymer nanostructure. Because faster polymerization kinetics can increase the degree of structure retained, polymerization was initiated using a low light intensity. Reducing the light intensity facilitated phase separation events and increased the sensitivity of the photo-DSC, allowing discontinuities in heat flow due to changes in local order to be identified.[23,31,36]

To demonstrate how photopolymerization kinetics can be utilized to identify changes in polymer morphology, two systems with significantly different morphologies before and after polymerization were chosen for detailed kinetic and structural characterization studies. Figure 2 shows the PLM images before and after polymerization for 20 wt % PEGDA with 50 wt % surfactant in water and 20 wt % HDDA with 50 wt % surfactant in water, referred to hereafter as PEGDA-50 and HDDA-50, respectively. These two systems were chosen for detailed analysis because each was found to markedly phase separate during polymerization. It is expected that a larger change in polymer structure will have a greater impact on photopolymerization kinetics, thus providing straightforward insight into the evolution of polymer structure.[33,35] A high birefringence and fan-like optical texture is observed before polymerization of PEGDA-50 (Figure 2a) and is indicative of a highly ordered hexagonal morphology.[43] However, after photopolymerization the birefringence decreases and the fan-like optical texture is less defined (Figure 2b), suggesting that the original hexagonal structure has not been retained during polymerization. Similarly, the Maltese cross optical texture and high birefringence of the HDDA-50 sample before polymerization (Figure 2c) indicates a well-defined lamellar morphology. Yet after polymerization, the original lamellar morphology is lost and a nearly isotropic polymer is obtained, indicated by the decrease in birefringence and ill-defined optical texture (Figure 2d).

To corroborate PLM results, the morphology of PEGDA-50 and HDDA-50 samples were characterized before and after polymerization using SAXS. Figure 3a shows the SAXS profile of PEGDA-50 before and after polymerization. The *d*-spacing ratios calculated from the SAXS profile of PEGDA-50 before polymerization is indicative of a highly ordered normal hexagonal morphology.[39] After polymerization, the scattering intensity decreases and the positions of the scattering peaks change, confirming that the structure of the PEGDA-50 polymer has been significantly disrupted during polymerization. A decrease in scattering intensity indicates a less ordered polymer due to the increased contribution of isotropic scatter to the invariant.[44,45] A similar analysis of SAXS profiles before and after polymerization for HDDA-50 (Figure 3b) supports that the original lamellar morphology is not retained during polymerization. The degree of phase separation is further illustrated by comparing the diffraction profile of a 5:3 weight ratio Brij 56−water solution shown in Figure 3a,b to the SAXS profile for the fully cured PEGDA-50 and HDDA-50 polymers. The Brij 56−water solution contains the same ratio of surfactant to water that would be present if the surfactant−water template completely phase separated from, and did not interact with, the PEGDA-50 or HDDA-50 polymers. The similar intensities and positions of the diffraction peaks of these SAXS profiles suggests that each polymer has phase separated to a large degree during polymerization and the resulting polymer structure is ill-defined and poorly ordered.

It is evident from PLM and SAXS data that the PEGDA-50 and HDDA-50 samples phase separate during polymerization. Utilizing photopolymerization kinetics, the critical conversion(s) at which the parent LLC template ceases to be thermodynamically stable may be identified. This was done by comparing the rate profiles of the PEGDA-50 and HDDA-50 samples to the rate profiles for the isotropic polymerization of the respective monomer in EGDAc to identify rate discontinuities that could signal the onset of phase separation. The sensitivity of the photo-DSC to changes in heat flow was increased by lowering the light intensity relative to kinetic studies presented in Figure 1. Discontinuities found in the rate profiles of LLC templated polymers and not in the rate profiles of

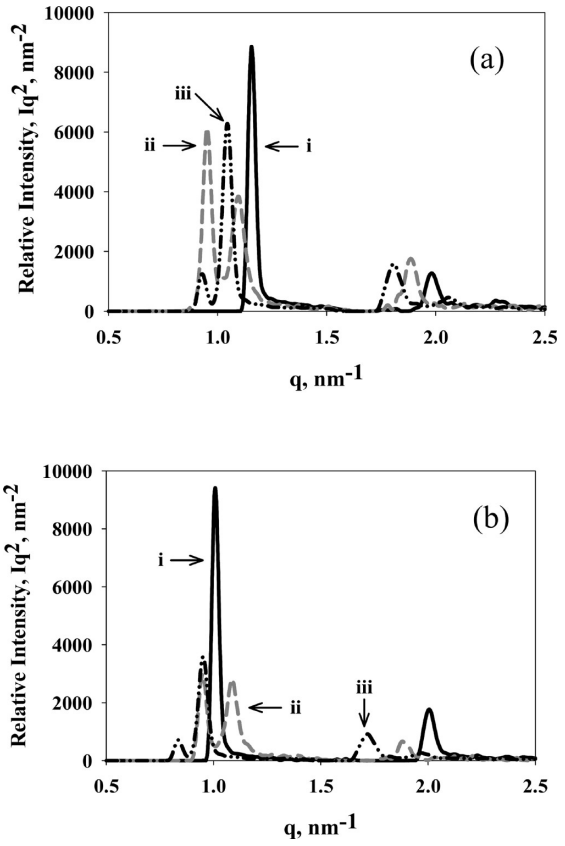

Figure 3. (a) SAXS profile of 20 wt % PEGDA with 50 wt % Brij 56 in water (normal hexagonal) before polymerization (i) and after polymerization (ii) as well as Brij 56-water mixture (iii) containing the same surfactant to water ratio. (b) SAXS profile for a 20 wt % HDDA with 50 wt % Brij 56 in water (lamellar) before polymerization (i) and after polymerization (ii) as well as Brij 56-water mixture (iii) containing the same surfactant to water ratio. Polymerization was initiated with 0.5 wt % Irgacure 651 at a light intensity of 0.5 mW/cm^2.

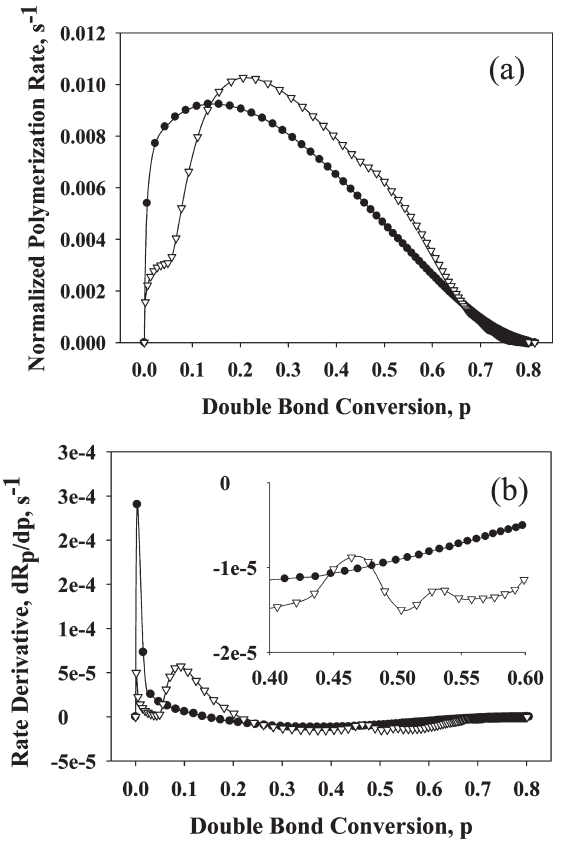

Figure 4. (a) Polymerization rate as a function of conversion of 20 wt % PEGDA in EGDAc (isotropic, ●) and with 50 wt % Brij 56 in water (normal hexagonal, ▽). (b) First derivative of polymerization rate shown in (a) with respect to conversion as a function of conversion of 20 wt % PEGDA in EGDAc (isotropic, ●) and with 50 wt % Brij 56 in water (normal hexagonal, ▽). The inset shows the rate derivative between 40 and 60% conversion. Polymerization was initiated with 0.5 wt % Irgacure 651 at a light intensity of 0.5 mW/cm^2.

isotropic controls are hypothesized to result from changes in monomer concentration, segregation, and diffusional behavior brought about by phase separation.[23,31,35,36] To test this hypothesis, the polymer morphology was characterized at double bond conversions near rate discontinuities to determine if such kinetic behavior coincides with changes in polymer structure. Polymers of specific double bond conversions were acquired by irradiating a sample in an aluminum DSC pan for an appropriate time and then closing the light shutter. Heat flow was monitored with photo-DSC and used to calculate double bond conversion. After the light shutter was closed, a steady baseline heat flow was established, the sample was removed from the DSC pan, placed into a lead sample holder, covered with X-ray transparent film (Mylar, DuPont), sealed with rubber O-rings, and the nanostructure was analyzed using SAXS. For clarity, the kinetic and structural analysis for PEGDA-50 and HDDA-50 samples will be presented separately.

Nanostructure Evolution of Hexagonal Templated PEGDA (PEGDA-50). To demonstrate how photopolymerization kinetics can be utilized to monitor the evolution of polymer nanostructure, the polymerization rate of anisotropic PEGDA-50 was compared to the polymerization rate of isotropic PEGDA in EGDAc to identify any rate discontinuities that could result from phase separation. Figure 4a shows the polymerization rate as a function of double bond conversion for PEGDA-50 and PEGDA in EGDAc. There are several differences between the rate profiles of the hexagonal templated PEGDA-50 sample and the isotropic PEGDA control. Specifically, polymerization rate discontinuities are observed in the first 10% conversion and between 40 and 55% conversion for the PEGDA-50 sample. The derivative of polymerization rate with respect to conversion, dR_p/dp, was calculated to reveal rate fluctuations that are not directly visible from the undifferentiated rate profile and is analogous to data analysis techniques used in Auger electron spectroscopy and X-ray photoelectron spectroscopy.[46] The rate derivative for the isotropic PEGDA control (Figure 4b) is rather smooth, indicating that there are no significant deviations in polymerization rate. However, there are several abrupt changes in the polymerization rate of PEGDA-50, illustrated by peaks in the rate derivative at 10, 45, and 55% double bond conversion.

Polymer nanostructures for double bond conversions preceding and following these rate discontinuities were characterized directly using SAXS to determine if rate fluctuations correspond to disruptions in polymer structure. Figure 5 summarizes the SAXS profiles obtained at conversions near the rate fluctuations shown in Figure 4b. A plateau in the polymerization rate was found in the rate profile of PEGDA-50 during the first 10% conversion and was not found in the rate profile for the isotropic PEGDA control. The SAXS profile at 15% conversion (Figure 5a) shows a decrease in intensity and shifts in the scattering peaks relative to the scattering profile obtained before polymerization, indicating that the original normal hexagonal morphology is significantly disrupted within the first 15% conversion.

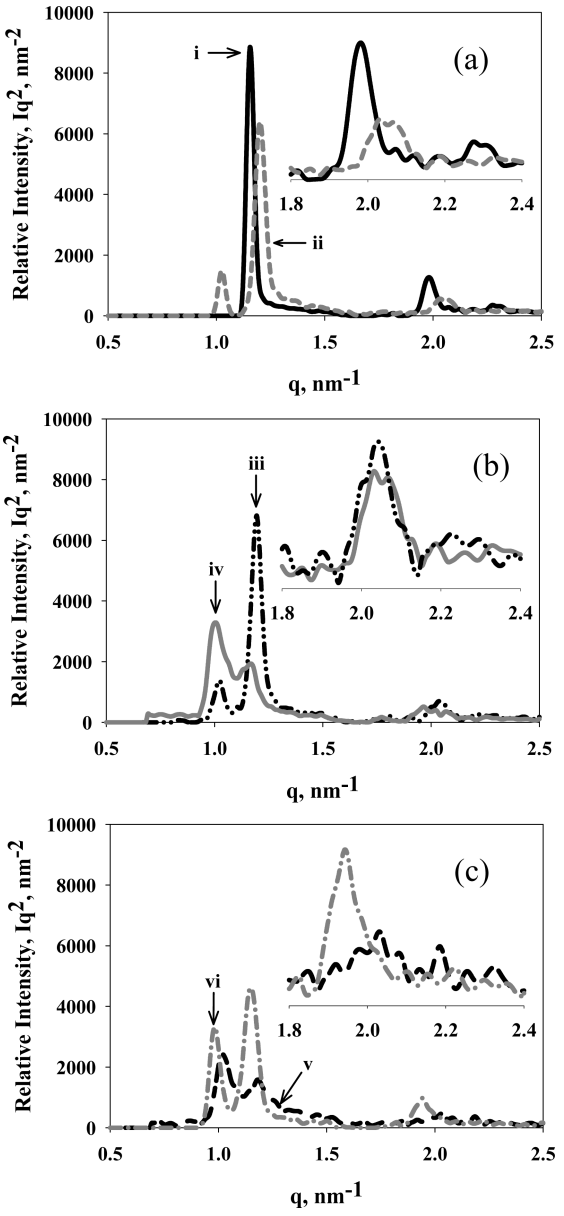

Figure 5. (a) SAXS profile for a 20 wt % PEGDA with 50 wt % Brij 56 in water (PEGDA-50, normal hexagonal) before polymerization (i) and at 15% conversion (ii), (b) 40% (iii) and 50% conversion (iv), and (c) 55% (v) and 70% conversion (vi). The insets show higher order scattering peaks. Polymerization was initiated with 0.5 wt % Irgacure 651 at a light intensity of 0.5 mW/cm^2.

Interestingly, this large disruption in PEGDA-50 polymer structure coincides with the rate plateau seen in Figure 4 during the first 10% conversion.

The rate derivative in Figure 4b decreases monotonically between 10 and 40% conversion for both the isotropic and anisotropic PEGDA samples. This indicates that the segregation behavior of double bonds has not been altered significantly between 10 and 40% conversion. Moreover, the absence of rate discontinuities suggests that no large changes in polymer structure have occurred. The scattering peaks in the SAXS profiles for PEGDA-50 at 15 and 40% conversion are very similar in position and intensity (Figure 5a,b), supporting that polymer morphology has not changed significantly between these conversions. On the other hand, the scattering profile at 50% conversion (Figure 5b) is much different from the profile observed at 40% conversion. Namely, the relative intensity of the secondary scattering peak at 50% conversion is much lower and the positions of the secondary and tertiary scattering peaks have shifted, indicating that a significant change in polymer morphology has occurred between 40 and 50% conversion. Furthermore, this change in polymer structure coincides with the rate discontinuity between 40 and 50% conversion shown in the inset of Figure 4b.

The structure of the PEGDA-50 polymer appears to evolve in a discrete manner with two significant phase separation events occurring during the first 50% conversion. Furthermore, disruptions in polymer structure appear to give rise to fluctuations in the polymerization rate. The inset of Figure 4b shows an additional rate fluctuation observed between 50 and 55% conversion. Comparison of the SAXS profiles at 50 and 55% conversion (Figure 5b,c) reveals a less defined tertiary scattering peak and a small decrease in intensity for the primary and secondary scattering peaks at 55% conversion. Thus, the rate fluctuation seen between 50 and 55% conversion coincides with a change in polymer morphology. The SAXS profile for PEGDA-50 at 70% conversion (Figure 5c) indicates that the structure continues to change. In fact, the scattering intensity increases and the tertiary scattering peak is more defined at 70% conversion compared to the SAXS profile at 55% conversion. Similar trends are observed during the final 10% double bond conversion. The scattering peaks for the fully cured PEGDA-50 polymer (Figure 3a) are well-defined and show an increase in scattering intensity relative to the SAXS profile at 70% conversion. It is unlikely that the PEGDA polymer is becoming more ordered at higher conversions because the network is highly cross-linked and structural rearrangement would require the breaking of covalent bonds.[23,32] Therefore, the increase in scattering intensity observed at 80% conversion is likely due to the self-assembly of surfactant and water into an ordered mesophase as a result of phase separation from the polymer network.

SAXS profiles at specific double bond conversions support that phase separation events occur in a stepwise manner for the PEGDA-50 polymer. For example, polymer structure changes significantly within the first 15% conversion, is similar between 15 and 40% conversion, is disrupted between 40 and 50% conversion, and is further altered between 50 and 55% conversion. Interestingly, significant disruptions in PEGDA-50 polymer nanostructure coincide with fluctuations in the polymerization rate shown in Figure 4b. Comparison of the SAXS profiles shown in Figure 5 reveal changes in the position and intensity of scattering peaks at conversions preceding and following rate discontinuities, supporting that disruption in polymer structure occurs in conjunction with rate discontinuities.

Nanostructure Evolution of Lamellar Templated HDDA (HDDA-50). The structural evolution of the HDDA-50 polymer was investigated to determine if photopolymerization kinetics could be used to identify disruptions in polymer structure during polymerization in a system having order and monomer segregation behavior different from those of the PEGDA-50 sample. The PLM images and SAXS profiles for HDDA-50 before and after polymerization indicate that the original lamellar morphology is lost during polymerization. Critical double bond conversions that may signal the onset of phase separation were identified by comparing the polymerization rate of the HDDA-50 sample to the isotropic polymerization rate of HDDA in solvent. Specifically, the HDDA-50 polymerization rate profile was analyzed for discontinuities not present in the rate profile of the isotropic HDDA control. Figure 6a,b

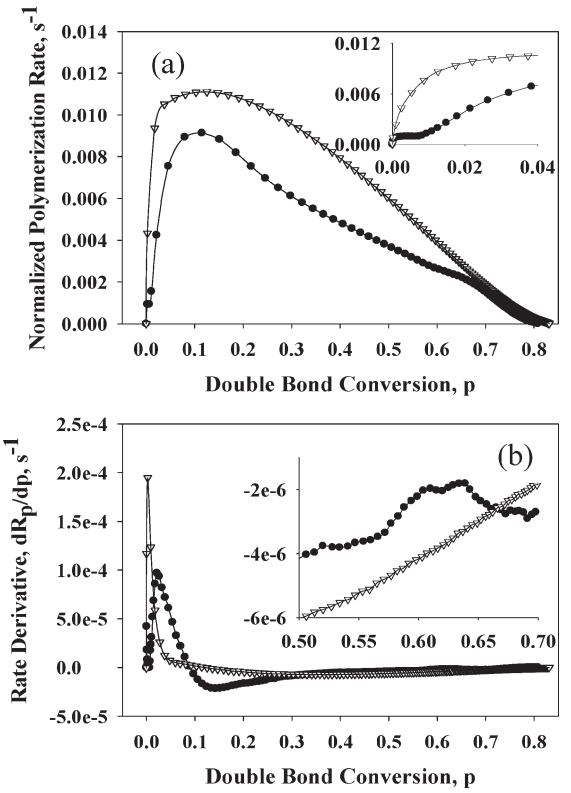

Figure 6. (a) Polymerization rate as a function of conversion for 20 wt % HDDA in EGDAc (isotropic, ▽) and with 50 wt % Brij 56 in water (lamellar, ●). The inset shows rate behavior at low conversion. (b) First derivative of the polymerization rate shown in (a) with respect to conversion as a function of conversion for 20 wt % HDDA in EGDAc (isotropic, ▽) and with 50 wt % Brij 56 in water (lamellar, ●). The inset shows the rate derivative between 50 and 70% conversion. Polymerization was initiated with 0.5 wt % Irgacure 651 at a light intensity of 0.5 mW/cm^2.

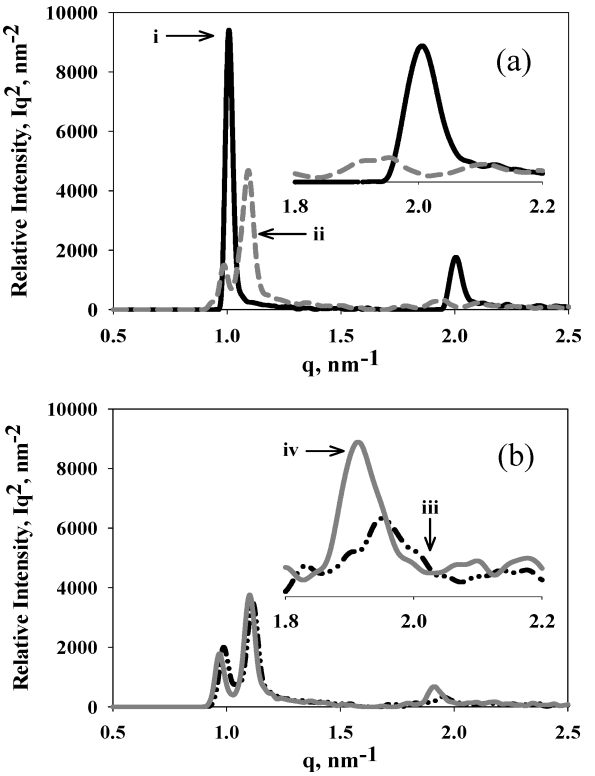

Figure 7. (a) SAXS profile for 20 wt % HDDA with 50 wt % Brij 56 in water (lamellar) before polymerization (i) and at 10% conversion (ii) and (b) at 55% conversion (iii) and at 65% conversion (iv). The insets show higher order scattering peaks. All polymerization were initiated with 0.5 wt % Irgacure 651 at a light intensity of 0.5 mW/cm^2.

show the polymerization rate as a function of double bond conversion and the rate derivative with respect to conversion for the HDDA-50 sample and isotropic HDDA control. Although the polymerization rate of HDDA-50 is similar to that of HDDA dissolved in EGDAc, there are several differences in the polymerization behavior of these systems. Two subtle rate discontinuities were found in the rate profile of the anisotropic HDDA-50 sample that are not present in the isotropic rate profile of HDDA in EGDAc. Specifically, a deceleration in polymerization rate is observed at very low conversions in the HDDA-50 sample, which is reflected as an initial rise and subsequent fall in the rate derivative shown in Figure 6b. It is unlikely that this shoulder is due to oxygen inhibition because samples were purged with nitrogen before polymerization and this behavior is not observed in the rate profile of the isotropic HDDA control.

The morphology of the partially polymerized HDDA-50 sample was characterized using SAXS at approximately 10% conversion that corresponds to the rate deceleration shown in the inset of Figure 6a. Figure 7a shows the SAXS profile for the HDDA-50 sample before polymerization and at 10% double bond conversion. It is evident from the SAXS profile for HDDA-50 at this conversion that the polymer structure is significantly disrupted early in the polymerization, indicated by a decrease in intensity and shifts in the diffraction peaks relative to the SAXS profile obtained before polymerization. Hence, the plateau in polymerization rate for HDDA-50 at low double bond conversion is accompanied by a significant change in polymer structure. The rate derivative for HDDA-50 and isotropic HDDA control (Figure 6b) is rather smooth between 10 and 55% conversion and no large changes in polymerization rate are observed. A smooth rate derivative was also seen for the PEGDA-50 and isotropic PEGDA control between 15 and 40% conversion (Figure 4b). In addition, the structure of the PEGDA-50 polymer was found to be very similar at 15 and 40% conversion, which suggests that no large change in structure has occurred between 10 and 55% conversion for the HDDA-50 sample. Comparison of the SAXS profile for HDDA-50 at 55% conversion (Figure 7b) to the SAXS profile at 10% conversion (Figure 7a) indicates that polymer structure has not changed significantly between these conversions. Specifically, the scattering intensities are similar and the positions of the diffraction peaks have not changed. Thus, the order of the HDDA-50 polymer has not been altered significantly between 10 and 55% conversion.

The polymerization kinetics and SAXS profiles for the PEGDA-50 and HDDA-50 systems show that rate fluctuations coincide with disruptions in polymer structure. From the results presented thus far, rate fluctuations appear to accompany significant changes in polymer structure. The subtle rate acceleration between 55 and 65% conversion shown in the inset of Figure 6b provides insight into the usefulness of photopolymerization kinetics in detecting small changes in polymer structure. The intensity of the tertiary scattering peak for HDDA-50 at 65% conversion (Figure 7b) is greater than at 55% conversion. Additionally, the positions of the tertiary peaks at 55 and 65% conversion are different, implying that the HDDA-50 polymer structure has been

disrupted between these conversions. The increase in intensity at 65% conversion is probably due to the self-assembly of surfactant and water into an ordered mesophase as a result of phase separation from the HDDA polymer.[23,32] Polymer structure continues to change during the final 15% conversion. The intensity of the primary and secondary scattering peaks is greater for the fully cured HDDA-50 polymer (Figure 3b) compared to the SAXS profile at 65% conversion. Although the polymer is not completely phase separated, the morphology has changed significantly throughout polymerization and the final structure of the HDDA-50 polymer is much different from the initial order of the parent LLC template.

The SAXS profiles of HDDA-50 at discrete double bond conversions support that disruptions in polymer structure coincide with fluctuations in polymerization rate. Specifically, a fluctuation in the polymerization rate was observed within the first 10% conversion and is accompanied by a significant change in polymer structure; no rate discontinuities or changes in polymer morphology are observed between 10% and 55% conversion; and a disruption in polymer structure coincides with the subtle rate discontinuity between 55 and 65% conversion. Polymer morphology does not appear to change substantially during the final 15% conversion with only slight decreases in order. These results demonstrate that photopolymerization kinetics are useful in monitoring the structural evolution of LLC templated polymers during polymerization and discontinuities in polymerization rate are primarily due to changes in polymer nanostructure.

Conclusions

Phase separation events of polymers templated in LLC mesophases were identified during polymerization by studying photopolymerization kinetics and characterizing polymer structure at specific conversions using SAXS. Several fluctuations were found in the polymerization rate of normal hexagonal templated PEGDA and lamellar templated HDDA monomers that were not present in the rate profiles of isotropic controls. A deceleration in polymerization rate was observed at low double bond conversions while rate accelerations are found at intermediate conversions during photopolymerization of the LLC templated mixtures. The nanostructure of anisotropic polymers was characterized using SAXS at conversions immediately preceding and following the observed rate discontinuities. SAXS data indicate that polymer structure is significantly different at conversions immediately following a rate fluctuation. These results support that polymerization rate discontinuities in LLC templated polymers result from phase separation events. Additionally, polymer structure was found to be very similar between conversions in which no rate discontinuities were present. Large changes in phase morphology appear to occur in conjunction with rate decelerations observed at low conversions. Additional changes in local order appear to coincide with rate accelerations found at intermediate conversions in the systems studied. These results show that photopolymerization kinetics can be used to identify changes in polymer nanostructure occurring during polymerization in LLC templates. This knowledge can be used to determine how LLC self-assembly and photopolymerization kinetics can be optimized to control polymer structure on the nanometer scale.

Acknowledgment. We thank The National Science Foundation for financial support of this project through CBET-0626395 and CBET-0933450 grants.

Note Added after ASAP Publication. This article posted ASAP on September 23, 2010 with an incorrect image for Figure 7. The correct version posted on September 28, 2010.

References and Notes

(1) Chung, H. J.; Park, T. G. *Nano Today* **2009**, *4*, 429–437.
(2) Wei, G.; Ma, P. X. *Adv. Funct. Mater.* **2008**, *18*, 3568–3582.
(3) Lu, X.; Nguyen, V.; Zeng, X.; Elliott, B. J.; Gin, D. L. *J. Membr. Sci.* **2008**, *318*, 397–404.
(4) Michler, G. H.; Balta-Calleja, F. J. *Mechanical Properties of Polymers based on Nanostructure and Morphology*; Taylor and Francis Group: Boca Raton, FL, 2005.
(5) Clapper, J. D.; Pearce, M. E.; Guymon, C. A.; Salem, A. K. *Biomacromolecules* **2008**, *9*, 1188–1194.
(6) Gin, D. L.; Bara, J. E.; Noble, R. D.; Elliott, B. J. *Macromol. Rapid Commun.* **2008**, *29*, 367–389.
(7) Clapper, J. D.; Guymon, C. A. *Macromolecules* **2007**, *40*, 1101–1107.
(8) Tsang, E. M. W.; Zhang, Z.; Yang, A. C. C.; Shi, Z.; Peckham, T. J.; Narimani, R.; Frisken, B. J.; Holdcroft, S. *Macromolecules* **2009**, *42*, 9467–9480.
(9) Yang, S. F.; Leong, K. F.; Du, Z. H.; Chua, C. K. *Tissue Eng.* **2001**, *7*, 679–689.
(10) Tierno, P.; Thonke, K.; Goedel, W. A. *Langmuir* **2005**, *21*, 9476–9481.
(11) Li, W.; Li, S. *Oligomers Polymer Composites Molecular Imprinting* **2007**, *206*, 191–210.
(12) Yoon, H.; Choi, M.; Lee, K. A.; Jang, J. *Macromol. Res.* **2008**, *16*, 85–102.
(13) Hentze, H. P.; Antonietti, M. *Curr. Opin. Solid State Mater. Sci.* **2001**, *5*, 343–353.
(14) Clapper, J. D.; Guymon, C. A. *Adv. Mater.* **2006**, *18*, 1575–1860.
(15) Sel, O.; Kuang, D. B.; Thommes, M.; Smarsly, B. *Langmuir* **2006**, *22*, 2311–2322.
(16) Adelhelm, P.; Hu, Y.; Chuenchom, L.; Antonietti, M.; Smarsly, B. M.; Maier, J. *Adv. Mater.* **2007**, *19*, 4012–4017.
(17) Liu, T. B.; Burger, C.; Chu, B. *Prog. Polym. Sci.* **2003**, *28*, 5–26.
(18) Antonietti, M.; Caruso, R. A.; Goltner, C. G.; Weissenberger, M. C. *Macromolecules* **1999**, *32*, 1383–1389.
(19) Clapper, J. D.; Sievens-Figueroa, L.; Guymon, C. A. *Chem. Mater.* **2008**, *20*, 768–781.
(20) Kumaraswamy, G.; Wadekar, M. N.; Agrawal, V. V.; Pasricha, R. *Polymer* **2005**, *46*, 7961–7968.
(21) Antonietti, M.; Basten, R.; Lohmann, S. *Macromol. Chem. Phys.* **1995**, *196*, 441–466.
(22) Hentze, H. P.; Kaler, E. W. *Curr. Opin. Colloid Interface Sci.* **2003**, *8*, 164–178.
(23) Lester, C. L.; Colson, C. D.; Guymon, C. A. *Macromolecules* **2001**, *34*, 4430–4438.
(24) Odian, G. *Principles of Polymerization*; John Wiley & Sons: Hoboken, NJ, 2004.
(25) Decker, C. *Polym. Int.* **2002**, *51*, 1141–1150.
(26) Kaur, M.; Srivastava, A. K. *J. Macromol. Sci., Polym. Rev* **2002**, *C42*, 481–512.
(27) DePierro, M. A.; Carpenter, K. G.; Guymon, C. A. *Chem. Mater.* **2006**, *18*, 5609–5617.
(28) Matuszewska-Czerwik, J.; Polwin′ski, S. *Eur. Polym. J.* **1991**, *27*, 743–746.
(29) Matuszewska-Czerwik, J.; Polwinski, S. *Eur. Polym. J.* **1990**, *26*, 549–552.
(30) DePierro, M. A.; Guymon, C. A. *Macromolecules* **2006**, *39*, 617–626.
(31) Guymon, C. A.; Hoggan, E. N.; Clark, N. A.; Rieker, T. P.; Walba, D. M.; Bowman, C. N. *Science* **1997**, *275*, 57–59.
(32) Lester, C. L.; Guymon, C. A. *Polymer* **2002**, *43*, 3707–3715.
(33) Lester, C. L.; Smith, S. M.; Jarrett, W. L.; Guymon, C. A. *Langmuir* **2003**, *19*, 9466–9472.
(34) Sievens-Figueroa, L.; Guymon, C. A. *Chem. Mater.* **2009**, *21*, 1060–1068.
(35) Sievens-Figueroa, L.; Guymon, C. A. *Polymer* **2008**, *49*, 2260–2267.
(36) Guymon, C. A.; Bowman, C. N. *Macromolecules* **1997**, *30*, 5271–5278.
(37) Anseth, K. S.; Wang, C. M.; Bowman, C. N. *Macromolecules* **1994**, *27*, 650–655.

(38) Singh, M. A.; Ghosh, S. S.; Shannon, R. F. *J. Appl. Crystallogr.* **1993**, *26*, 787–794.
(39) Feigin, L. A.; Svergun, D. I. In *Structure Analysis by Small Angle X-Ray and Neutron Scattering*, Taylor, G., Ed.; Plenum Press: New York, NY, 1987; pp 59−63.
(40) Glatter, O.; Kratky, O. In *Small Angle X-ray Scattering*; Porod, G., Ed.; General Theory; Academic Press Inc.: New York, NY, 1982.
(41) Cser, F. *J. Appl. Polym. Sci.* **2001**, *80*, 2300–2308.
(42) Andrzejewska, E. *Prog. Polym. Sci.* **2001**, *26*, 605–665.
(43) Collings, P. J.; Hird, M. *Introduction to Liquid Crystals: Chemistry and Physics*; Taylor & Francis, Inc.: Philadelphia, PA, 1997.
(44) Junker, M.; Walther, J.; Braun, D.; Alig, I. *Angew. Makromol. Chem.* **1997**, *250*, 119–131.
(45) Page, K. A.; Landis, F. A.; Phillips, A. K.; Moore, R. B. *Macromolecules* **2006**, *39*, 3939–3946.
(46) Briggs, D.; Seah, M. P. *Practical Surface Analysis by Auger and X-ray Photoelectron Spectroscopy*; Wiley: New York, NY, 1983.